

Monoamine Oxidase Inhibitory Activity: Methyl- versus Chloroalcone Derivatives

Bijo Mathew^{+, * [a]}, Gülberk Uçar^{+, * [b]}, Githa Elizabeth Mathew,^[c] Sincy Mathew,^[d] Praseedha Kalatharakal Purapurath,^[d] Fasil Moolayil,^[d] Smrithy Mohan,^[d] and Sheeba Varghese Gupta^[e]

Numerous studies have shown that chalcones are promising scaffolds for the development of new monoamine oxidase-B (MAO-B) inhibitors. As a continuation of our ongoing research into the development of reversible human MAO-B (hMAO-B) inhibitors, two series of twenty chalcones containing electron-donating and electron-withdrawing substituents were synthesized. All compounds were found to be competitive, selective, and reversible inhibitors of hMAO-B except (2*E*)-1-(4-methylphenyl)-3-(4-nitrophenyl)prop-2-en-1-one (**P7**) and (2*E*)-1-(4-chlorophenyl)-3-(4-nitrophenyl)prop-2-en-1-one (**P17**), which were found to be selective inhibitors of hMAO-A. The most potent hMAO-B inhibitor, (2*E*)-1-(4-chlorophenyl)-3-(4-ethylphenyl)prop-2-en-1-one (**P16**), showed a K_i value of $0.11 \pm 0.01 \mu\text{M}$. Molecular docking simulations were carried out to identify the hypothetical binding mode for the most potent compounds in the active sites of hMAO-A and B. The ability of the compounds to cross the blood–brain barrier was assessed by parallel artificial membrane permeability assay (PAMPA). Additionally, the most potent hMAO-B inhibitor **P16** showed no toxicity in cultured hepatic cells at concentrations of 5 and 25 μM .

Monoamine oxidase inhibitors (MAOIs) have been extensively studied because of their role in the treatment of psychiatric and neurological disorders. The first generation of MAOIs were nonselective and irreversible, with serious side effects such as liver toxicity and hypertensive crisis. This led to their withdrawal from clinical use.^[1] Based on the catalytic activities of the MAO-A and MAO-B isoforms, MAO-A has been considered

a drug target to treat depression and anxiety disorders.^[2] As MAO-B appears to be the major dopamine-metabolizing enzyme in the basal ganglia, selective MAO-B inhibitors are used in the treatment of neurodegenerative disorders such as idiopathic Parkinson's disease (PD).^[3,4] Irreversible MAO-B inhibitors in current use covalently bind their target, rendering the enzyme functionless; MAO-B activity is therefore blocked until the cell produces more enzyme. Reversible inhibitors have the capacity to detach from their target enzyme, to facilitate normal substrate catabolism.^[5] There is an urgent need for reversible MAO-B inhibitors with safe side-effect profiles for use as an adjunct to L-DOPA therapy for the treatment of PD.

Elevated central nervous system (CNS) levels of MAO-B in PD patients leads to an increased production of hydrogen peroxide and reactive oxygen species.^[6,7] These toxic metabolites are responsible for neurodegeneration, leading to the death of dopamine-containing neurons. Depletion of dopamine is responsible for the major motor symptoms associated with PD.^[8] Notable MAO-B-selective and irreversible inhibitors such as selegiline and rasagiline are approved for PD monotherapy, or as adjunctive therapies to L-DOPA.^[9] Safinamide, a reversible MAO-B-selective inhibitor, has completed phase III trials for the treatment of PD.^[10] Clinical trials of another MAO-B inhibitor, lazabemide, have been discontinued due to reports of liver toxicity.^[11,12] Some studies have suggested that MAO-B inhibitors with neuroprotective properties can be used as an ancillary treatment for Alzheimer's disease (AD).^[13] The design and development of new multifunctional MAO-B inhibitors for the treatment of PD and AD appears to be a promising course.

Chemically, chalcones are 1,3-diphenyl-2-propen-1-ones, consisting of two aromatic rings (rings A and B) with a double bond in conjugation with a carbonyl group.^[14] Many studies have shown that these scaffolds have selective and reversible/irreversible MAO-B inhibitory activity in the nanomolar range.^[15–21] Prior studies revealed that the removal of the double bond system in chalcone leads to decreased activity in MAO inhibition.^[22,23] Additionally, heterocyclic substituents such as furan, chromene, thiophene, piperidine, quinoline, and indole in the chalcone scaffold lead to improved MAO inhibition.^[24–32] Recent reports have shown that chalcones are more potent inhibitors of MAO-A than of MAO-B. This selectivity may be due to steric hindrance and the nature and orientation of functional groups on the phenyl ring of chalcones.^[33,34] The presence of lipophilic groups such as ethyl, methyl, dimethylamino, bromo, chloro, fluoro, and trifluoromethyl groups at the *para* position of ring B increases MAO-B inhibitory activity. Lip-

[a] Dr. B. Mathew⁺

Division of Drug Design and Medicinal Chemistry Research, Department of Pharmaceutical Chemistry, Ahalia School of Pharmacy, Palakkad 678557 Kerala (India)
E-mail: bijovilaventgu@gmail.com

[b] Prof. Dr. G. Uçar⁺

Department of Biochemistry, Faculty of Pharmacy, Hacettepe University, Sıhhiye, 06100 Ankara (Turkey)
E-mail: gulberk@hacettepe.edu.tr

[c] G. E. Mathew

Department of Pharmacology, Grace College of Pharmacy, Palakkad 678004, Kerala (India)

[d] S. Mathew, P. Kalatharakal Purapurath, F. Moolayil, S. Mohan

Department of Pharmaceutical Chemistry, Grace College of Pharmacy, Palakkad 678004, Kerala (India)

[e] Dr. S. Varghese Gupta

Department of Pharmaceutical Sciences, College of Pharmacy, University of South Florida, Tampa, FL 33612 (USA)

[†] These authors contributed equally to this work.

ophilic groups favor interaction with the entrance cavity in the MAO-B active site. Molecular modeling studies of chalcones in the hMAO-B active site have shown that ring A is oriented toward the FAD cofactor and is stabilized by both hydrophobic and hydrogen bonding interactions.^[21] We recently reported the synthesis and evaluation of aryl/heteroarylchalcones as selective MAO-B inhibitors (Figure 1).^[18,20,29–32] In continuation of

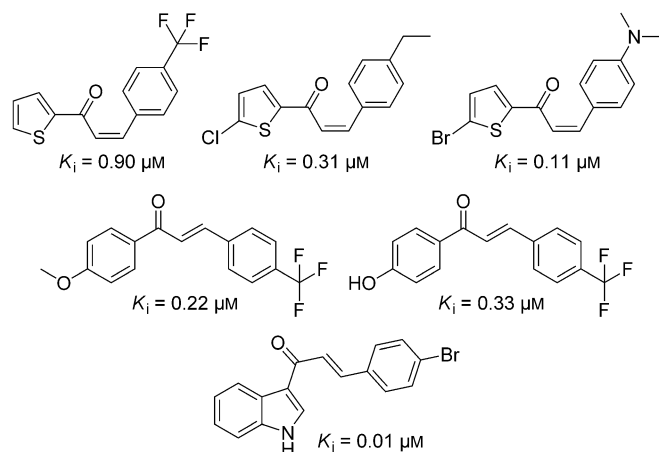
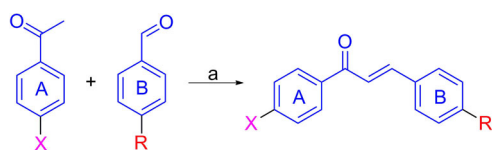


Figure 1. Recently reported aryl/heteroarylchalcone-based MAO-B inhibitors from our research group.^[18,20,29–32]

this work, herein we report the design, synthesis, and MAO inhibitory activities of methyl- and chloro-based chalcones. To diversify the chalcone structures and investigate the possible structure–activity relationship (SAR), we introduced lipophilic substituents such as chloro and methyl at the *para* position of ring A, and various electron-donating and -withdrawing groups at the *para* position of phenyl ring B.

Chalcones were synthesized by Claisen–Schmidt condensation between *para*-substituted acetophenones and various aromatic aldehydes in the presence of 40% potassium hydroxide as base in ethanol with stirring at room temperature for 2–6 h (Scheme 1). The resulting product was kept overnight at 4 °C.



Scheme 1. Synthetic route toward methoxy-substituted chalcones. Reagents and conditions: a) C₂H₅OH, 40% KOH, RT, stirring, 4–6 h.

The resulting precipitate was filtered, washed with water, and recrystallized from ethanol. Products were characterized by ¹H and ¹³C NMR spectroscopy and mass spectrometry.

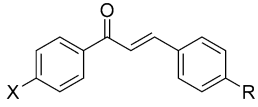
The newly synthesized chalcones were screened for their inhibitory activities toward recombinant human MAO isoforms. Enzyme activities were determined according to a previously reported method using the Amplex Red MAO assay kit.^[35–37]

The assay procedure provides a one-step fluorimetric method for the continuous measurement of MAO activity using a fluorescence microplate reader. The assay is based on the detection of hydrogen peroxide in a horseradish-peroxidase-coupled reaction using the highly sensitive Amplex Red reagent. The reaction product, resorufin, is highly stable and easily detectable. Chalcones and reference inhibitors (moclobemide and selegiline) did not show any interference with the detection of resorufin at the absorption and fluorescence wavelengths (λ 571 and 585 nm, respectively). *p*-Tyramine (0.05–0.50 mM) was used as the substrate for both hMAO-A and hMAO-B.

Specific enzyme activities were calculated as $149.55 \pm 6.08 \text{ pmol mg}^{-1} \text{ min}^{-1}$ ($n=3$) for hMAO-A and $136.88 \pm 5.00 \text{ pmol mg}^{-1} \text{ min}^{-1}$ ($n=3$) for hMAO-B. The K_i values for the inhibition of MAOs by the chalcones are listed in Table 1. The selectivity index (SI) is given as the ratio of $K_{i(\text{MAO-A})}/K_{i(\text{MAO-B})}$. Selectivity for MAO-A increases as the SI value decreases, whereas selectivity toward the MAO-B isoform increases with increasing SI. All chalcones were found to be competitive, selective, and reversible toward hMAO-B except (2*E*)-1-(4-methylphenyl)-3-(4-nitrophenyl)prop-2-en-1-one (**P7**) and (2*E*)-1-(4-chlorophenyl)-3-(4-nitrophenyl)prop-2-en-1-one (**P17**), which were selective inhibitors of hMAO-A with K_i values of 0.41 and 0.18 μM , respectively. Experimental SI values for these compounds were calculated as 0.26 and 0.13, respectively.

This showed that the presence of a nitro group on the chalcone ring B can produce a shift in the MAO-A inhibitory activity. The same trend was observed in our previous hMAO inhibition studies on chlorinated and brominated thienyl chalcones.^[30,31] The results show that chloro substitution on ring A is more favorable for MAO-B inhibition than methyl substitution. The most potent MAO-B inhibitor, (2*E*)-1-(4-chlorophenyl)-3-(4-ethylphenyl)prop-2-en-1-one (**P16**), exhibited a K_i value of $0.11 \pm 0.01 \mu\text{M}$ with an SI of 16. It was found to be better than the standard drug selegiline (hMAO-B $K_i=0.35 \pm 0.01 \mu\text{M}$) with a selectivity index of 15.8. From the inhibition data, some crucial SARs can be derived. The introduction of halogen atoms at the *para* position of ring B yielded some interesting results. In both series of chalcones, bromine substitution led to more potent compounds (**P9**: $K_i=0.20 \mu\text{M}$, **P19**: $K_i=0.16 \mu\text{M}$). On the other hand, substitution with fluorine produced a less potent MAO-B inhibitor than chlorine and bromine substituents in both series of chalcones. Properties such as atomic radius and/or electronegativity may therefore play a significant role in the ligand–enzyme interaction.^[38]

Electron-donating substituents such as ethyl and methoxy groups in chlorine-containing chalcones have a significant influence on hMAO-B inhibition; for example, compounds **P16** and **P13** were found to be better in terms of potency and selectivity than the corresponding compounds **P1** and **P11** without these substituents. In particular, methoxy-substituted compound **P13** showed a K_i value of $0.22 \pm 0.01 \mu\text{M}$ with SI = 37.55; this SI is much higher than that of the standard selegiline. The chlorine atom at the *para* position of ring A appears to be ideal for potent hMAO-B inhibition. The introduction of a hydroxy group at the *para* position of ring B results in 5- to 9-fold lower hMAO-B inhibitory activity than **P16**. The presence

Table 1. Monoamine oxidase inhibitory activity of chalcones.


Compound	X	R	Exptl. K_i [μM] ^[a]		Exptl. SI ^[b]	Inhibition type	Reversibility	Selectivity
			MAO-A	MAO-B				
P1	Me	H	4.06 ± 0.19	1.45 ± 0.11	2.80	competitive	reversible	MAO-B
P2	Me	OH	3.62 ± 0.20	1.02 ± 0.09	3.55	competitive	reversible	MAO-B
P3	Me	OMe	1.95 ± 0.15	0.88 ± 0.05	2.22	competitive	reversible	MAO-B
P4	Me	Me	1.90 ± 0.12	0.46 ± 0.02	4.13	competitive	reversible	MAO-B
P5	Me	N(Me) ₂	1.44 ± 0.11	0.29 ± 0.01	4.97	competitive	reversible	MAO-B
P6	Me	Et	0.88 ± 0.04	0.47 ± 0.01	1.87	competitive	reversible	MAO-B
P7	Me	NO ₂	0.41 ± 0.01	1.55 ± 0.10	0.26	competitive	reversible	MAO-A
P8	Me	Cl	1.26 ± 0.10	0.30 ± 0.02	4.20	competitive	reversible	MAO-B
P9	Me	Br	1.44 ± 0.12	0.20 ± 0.01	7.20	competitive	reversible	MAO-B
P10	Me	F	4.09 ± 0.23	0.97 ± 0.03	4.22	competitive	reversible	MAO-B
P11	Cl	H	2.85 ± 0.17	0.47 ± 0.01	6.06	competitive	reversible	MAO-B
P12	Cl	OH	1.78 ± 0.14	0.66 ± 0.03	2.70	competitive	reversible	MAO-B
P13	Cl	OMe	8.26 ± 0.57	0.22 ± 0.01	37.55	competitive	reversible	MAO-B
P14	Cl	Me	1.67 ± 0.12	0.31 ± 0.01	5.39	competitive	reversible	MAO-B
P15	Cl	N(Me) ₂	1.46 ± 0.11	0.42 ± 0.02	3.48	competitive	reversible	MAO-B
P16	Cl	Et	1.76 ± 0.12	0.11 ± 0.01	16.00	competitive	reversible	MAO-B
P17	Cl	NO ₂	0.18 ± 0.01	1.36 ± 0.11	0.13	competitive	reversible	MAO-A
P18	Cl	Cl	1.22 ± 0.09	0.20 ± 0.01	6.10	competitive	reversible	MAO-B
P19	Cl	Br	0.97 ± 0.04	0.16 ± 0.01	6.06	competitive	reversible	MAO-B
P20	Cl	F	1.74 ± 0.11	0.66 ± 0.04	2.64	competitive	reversible	MAO-B
moclobemide	–	–	0.15 ± 0.01	1.77 ± 0.12	0.08	competitive	reversible	MAO-A
selegiline	–	–	5.55 ± 0.21	0.35 ± 0.01	15.86	suicide	irreversible	MAO-B

[a] Values are the mean ± SEM ($n=3$). [b] Selectivity index (SI) was calculated as $K_{i(\text{MAO-A})}/K_{i(\text{MAO-B})}$; selectivity toward the MAO-A isoform increases as the corresponding SI decreases, whereas selectivity toward the MAO-B isoform increases as the corresponding SI increases.

of a hydrophilic substituent was not well tolerated in ring B; this may affect the recognition of the hydrophobic pocket of MAO. Our SARs therefore reveal that electron-donating groups such as ethyl or methoxy and a lipophilic bromine atom result in more potent MAO-B inhibitory activity than electron-withdrawing substituents at the chalcone ring B.

For kinetics experiments, the catalytic rates of hMAO-A and hMAO-B activity at various *p*-tyramine concentrations were measured for the most potent MAO-A inhibitor (**P17**) and MAO-B inhibitor (**P16**) from this series. Lineweaver–Burk plots were constructed in the absence of inhibitor, and in the presence of various reference compounds and new inhibitors. The set consisted of six graphs, each plotted by measuring MAO-A and MAO-B catalytic rates at various substrate concentrations. The first Lineweaver–Burk plot was generated in the absence of inhibitor, and the remaining five traces were plotted in the presence of various concentrations of **P17** (0.05–0.60 μM) and **P16** (0.1–1.2 μM). As the lines intersect at the *y* axis, it can be inferred that **P17** and **P16** are competitive inhibitors of hMAO-A and hMAO-B (Figures 2 and 3). Replots of the slopes of the Lineweaver–Burk plots versus inhibitor concentrations are shown in Figures 4 and 5, and the K_i values were estimated to be 0.18 and 0.11 μM for **P17** (hMAO-A) and **P16** (hMAO-B), respectively. Protein concentration was determined according to the Bradford method.^[39]

The reversibility of MAO inhibition by chalcones was investigated by determining the recoveries of MAO activities after di-

alysis of enzyme–inhibitor mixtures. MAO isoforms were incubated in the presence of the inhibitors at concentrations equal to $4 \times \text{IC}_{50}$ values for a period of 15 min and subsequently dialyzed for 24 h.^[40] The results of the reversibility tests of chalcones on both hMAO isoforms are listed in Table 2. The data suggest that these new compounds are reversible inhibitors of both hMAO isoforms. The compounds have considerable advantages over irreversible inhibitors, which, as mentioned above, may possess serious pharmacological side effects. The reversibility of compound **P17** (hMAO-A) was calculated as 35.11 ± 1.90 and $95.10 \pm 4.22\%$ before and after dialysis, respectively, whereas the percent inhibition of hMAO-A by moclobemide was calculated as 39.10 ± 1.12 and $92.25 \pm 4.01\%$ before and after dialysis, respectively. At the same time, compound **P16** exhibited good reversibility in hMAO-B inhibition. The reversibility values for **P16** was calculated as 32.11 ± 1.14 and $95.55 \pm 3.89\%$ before and after dialysis, respectively. The reversible nature of **P16** imparts it with considerable advantages over the irreversible inhibitor selegiline, with 56.29 ± 2.65 and $57.00 \pm 1.98\%$ reversibility before and after dialysis.

To explore the hypothetical binding interaction modes of compound **P17** (Figure 6) with hMAO-A and compound **P16** with hMAO-B (Figure 7), docking studies were performed by using the AutoDock 4.2 software package.^[41] Many researchers have preferred to use the crystallographic coordinates of MAO co-crystallized with noncovalent ligands (PDB IDs: 2Z5X, 2V60, 2V5Z 2BK3),^[42,43] but the experimental and predicted inhibition

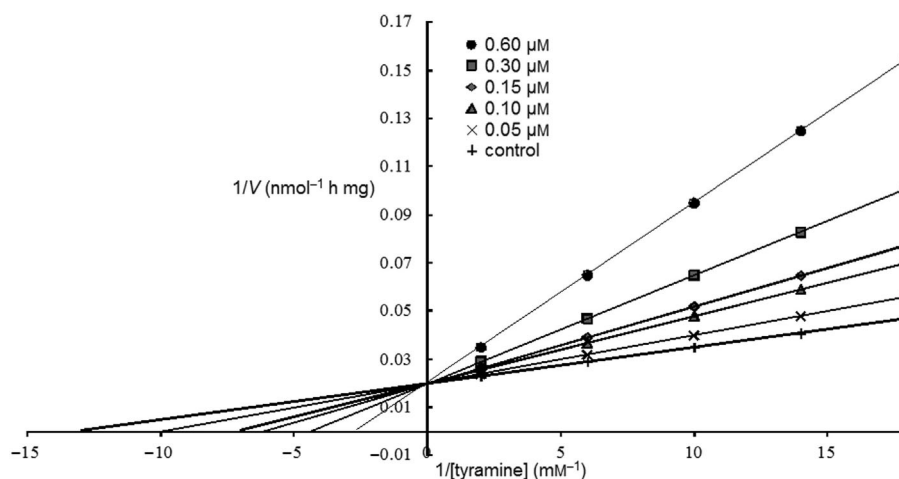


Figure 2. Lineweaver–Burk plots of the oxidation of *p*-tyramine by recombinant hMAO-A. The plots were constructed in the absence and in the presence of various concentrations of compound P17.

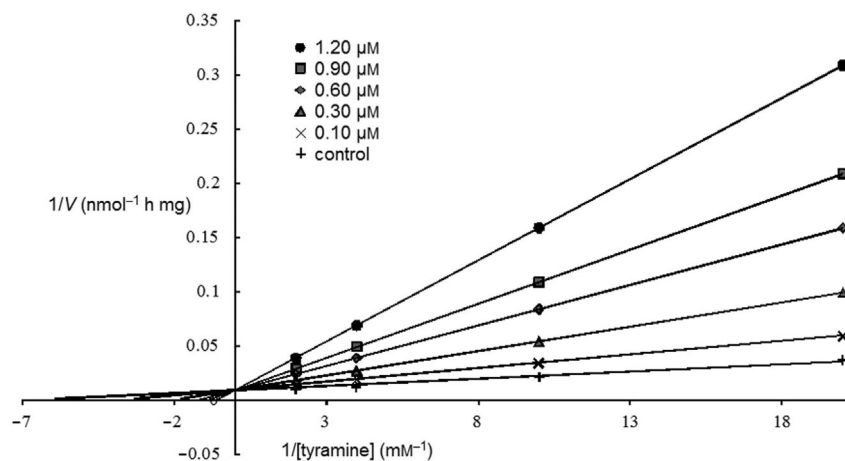


Figure 3. Lineweaver–Burk plots of the oxidation of *p*-tyramine by recombinant hMAO-B. The plots were constructed in the absence and in the presence of various concentrations of compound P16.

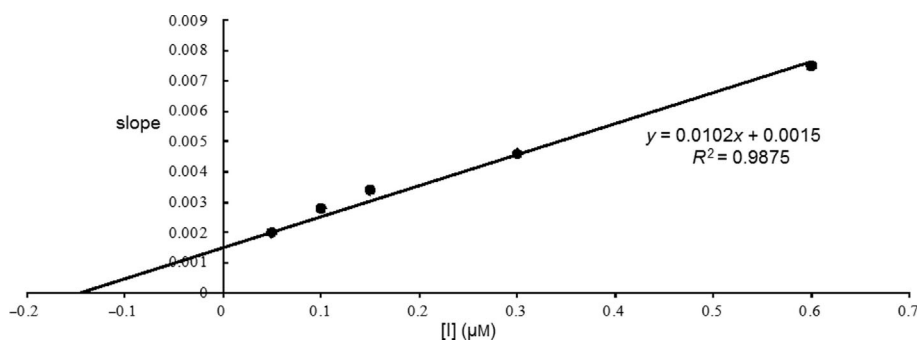


Figure 4. Replots of the slopes of the Lineweaver–Burk plots versus inhibitor P17 concentration (hMAO-A).

constant (K_i) values did not correlate well in our studies. Hence, we adopted an earlier protocol reported by our group with PDB IDs: 2BXR and 2BYB.^[44–46] Protein and ligand preparation was carried out according to previously reported methods.^[47,48]

Compound P17 is mainly stabilized by hydrogen bonding and π – π stacking interactions with the inhibitor binding cavity (IBC) of hMAO-A outlined by such residues as Tyr69, Pro72, Gln 74, Ser209, Glu 216, Arg 296, Trp441, Tyr444, and the isoal-

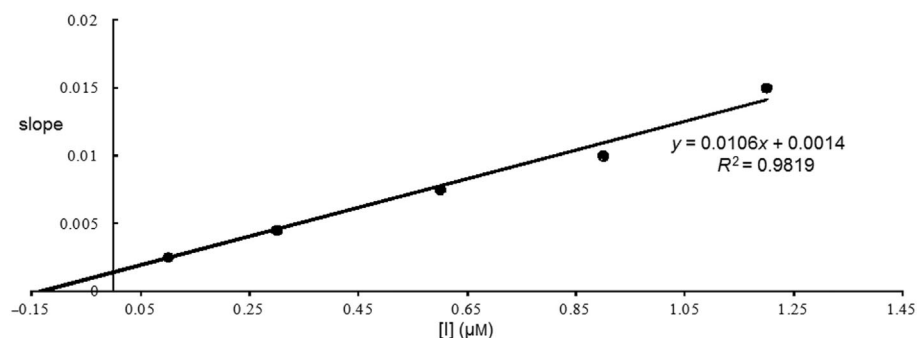


Figure 5. Replots of the slopes of the Lineweaver–Burk plots versus inhibitor **P16** concentration (hMAO-B).

Compound	hMAO-A activity [%] ^[a]		hMAO-B activity [%] ^[a]		Reversibility
	Before dialysis	After dialysis	Before dialysis	After dialysis	
No inhibitor	100 ± 0.00	100 ± 0.00	100 ± 0.00	100 ± 0.00	–
moclobemide	39.10 ± 1.12	92.25 ± 4.01	90.30 ± 3.87	93.00 ± 5.03	reversible
selegiline	90.25 ± 2.55	94.25 ± 5.23	56.29 ± 2.65	57.00 ± 1.98	irreversible
lazabemide	91.20 ± 3.68	96.00 ± 4.75	15.11 ± 1.02	89.80 ± 4.01	reversible
P1	90.11 ± 5.22	97.16 ± 4.77	66.75 ± 2.10	91.29 ± 3.13	reversible
P2	85.49 ± 2.17	98.00 ± 5.22	60.49 ± 2.34	91.55 ± 3.72	reversible
P3	82.26 ± 2.13	98.44 ± 4.22	54.55 ± 1.74	88.70 ± 4.00	reversible
P4	88.00 ± 4.12	95.54 ± 3.21	48.00 ± 1.77	92.22 ± 3.50	reversible
P5	84.77 ± 3.76	90.11 ± 2.54	38.88 ± 2.16	95.29 ± 4.76	reversible
P6	89.78 ± 4.00	96.99 ± 3.56	44.55 ± 1.97	88.23 ± 1.90	reversible
P7	48.22 ± 2.64	89.96 ± 3.80	87.22 ± 4.19	97.00 ± 5.16	reversible
P8	84.22 ± 3.11	92.57 ± 4.00	38.22 ± 2.18	94.55 ± 2.80	reversible
P9	81.85 ± 5.00	96.00 ± 4.70	37.00 ± 1.55	92.21 ± 3.80	reversible
P10	89.00 ± 3.77	95.99 ± 4.61	62.77 ± 2.16	98.00 ± 4.05	reversible
P11	88.40 ± 3.11	95.33 ± 3.19	51.20 ± 1.33	94.44 ± 2.74	reversible
P12	85.22 ± 3.13	97.10 ± 4.55	54.55 ± 2.19	90.60 ± 3.98	reversible
P13	88.00 ± 2.16	95.88 ± 3.55	35.14 ± 1.18	91.22 ± 3.49	reversible
P14	79.30 ± 3.47	93.00 ± 4.19	40.16 ± 2.60	93.00 ± 4.45	reversible
P15	84.55 ± 2.90	96.44 ± 3.08	44.80 ± 2.33	88.22 ± 2.60	reversible
P16	88.45 ± 3.25	92.22 ± 4.11	32.11 ± 1.44	95.55 ± 3.89	reversible
P17	35.51 ± 1.90	95.10 ± 4.22	88.27 ± 3.55	92.25 ± 4.55	reversible
P18	89.00 ± 4.06	95.78 ± 3.20	36.55 ± 1.27	90.19 ± 3.77	reversible
P19	88.46 ± 4.13	97.00 ± 4.05	33.25 ± 1.98	94.01 ± 3.47	reversible
P20	84.29 ± 2.81	90.08 ± 4.33	55.78 ± 2.75	90.66 ± 3.41	reversible

[a] Values are the mean ± SEM (n = 3).

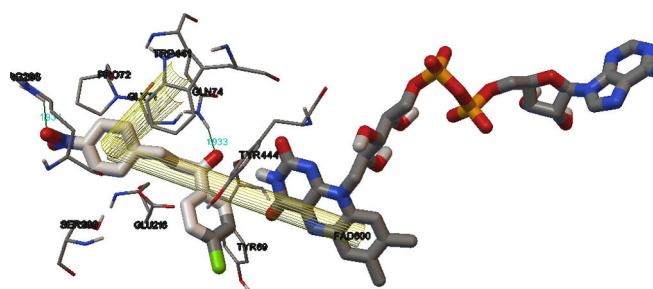


Figure 6. Docking pose of **P17** in the MAO-A active site: yellow mesh indicates π - π stacking interactions.

loxazine ring of FAD. In this pose, the sp^2 -hybridized carbonyl oxygen atom and the nitro group of the chalcone make hydrogen bonds with Gln74 (1.933 Å) and Arg298 (1.933 Å), respec-

tively. The electron-withdrawing nitro group at the chalcone ring B makes strong π - π stacking interactions to Trp441 and the FAD cofactor of hMAO-A. These interactions are therefore likely to contribute to the placement of **P17** within the IBC of hMAO-A (Figure 6).

The binding mode of the potent hMAO-B inhibitor **P16** is shown in Figure 7. The chloro-substituted ring A is positioned between the Tyr435 and Tyr398 aromatic cage stabilized by π - π stacking interactions. This position satisfies the minimal distance between the chlorine atom and N5 of the FAD unit. Because the entrance cavity of hMAO-B is reported to be a highly hydrophobic space,^[49] it may be expected that an enhancement of the lipophilicity of the ethyl substituent on ring B of the chlorinated chalcone will result in more productive van der Waals interactions with the entrance cavity, and therefore an enhancement in binding affinity.

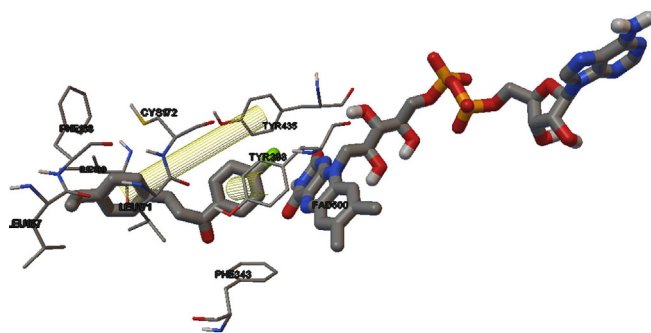


Figure 7. Docking pose of **P16** in the MAO-B active site; yellow mesh indicates π - π stacking interactions.

The CNS effectiveness of the target compounds greatly depends on their capacity to cross the blood–brain barrier (BBB).^[50] A parallel artificial membrane permeation assay of the blood–brain barrier (PAMPA–BBB) was used to determine whether these chalcones can pass this barrier.^[51] Assay validation was made by comparing experimental permeabilities of nine commercial drugs with reported values (Table 3). The data

Table 3. Experimental permeability values of chalcones and of commercial drugs used in assay validation.

Compound ^[a]	P_e [$\times 10^{-6} \text{ cm s}^{-1}$] ^[b]		Prediction
	Published ^[51]	Experimental	
testosterone	17.0	17.22 ± 1.11	CNS +
verapamil	16.0	15.88 ± 1.20	CNS +
β -estradiol	12.0	11.33 ± 0.99	CNS +
progesterone	9.3	8.76 ± 0.30	CNS +
corticosterone	5.1	5.21 ± 0.19	CNS +
piroxicam	2.5	2.60 ± 0.16	CNS +/–
hydrocortisone	1.8	1.71 ± 0.66	CNS –
lomefloxacin	1.1	1.07 ± 0.02	CNS –
dopamine	0.2	0.22 ± 0.01	CNS –
P1	–	6.17 ± 0.34	CNS +
P2	–	7.20 ± 0.44	CNS +
P3	–	9.33 ± 0.37	CNS +
P4	–	8.22 ± 0.50	CNS +
P5	–	8.85 ± 0.39	CNS +
P6	–	6.45 ± 0.41	CNS +
P7	–	8.57 ± 0.21	CNS +
P8	–	9.00 ± 0.37	CNS +
P9	–	11.17 ± 0.96	CNS +
P10	–	5.90 ± 0.19	CNS +
P11	–	7.88 ± 0.67	CNS +
P12	–	9.60 ± 0.74	CNS +
P13	–	15.70 ± 0.70	CNS +
P14	–	7.64 ± 0.40	CNS +
P15	–	10.00 ± 0.90	CNS +
P16	–	14.11 ± 0.75	CNS +
P17	–	10.27 ± 0.95	CNS +
P18	–	9.27 ± 0.47	CNS +
P19	–	8.16 ± 0.55	CNS +
P20	–	6.90 ± 0.36	CNS +

[a] Compounds were dissolved in DMSO at 5 mg mL⁻¹ and diluted with PBS/EtOH (70:30); final compound concentration was 100 μ g mL⁻¹. [b] Determined by PAMPA–BBB assay; values are the mean \pm SD of three independent experiments.

indicate that all the derivatives can cross the BBB to target the enzyme in the CNS. Compounds **P9**, **P13**, and **P16** showed the highest permeability, suggesting that they may cross the BBB easily and reach the biological targets located in the CNS, which are consistent with our design strategy.

The in vitro cytotoxicity of these chalcones was tested in HepG2 cells at three different concentrations (1–25 μ M; Table 4). The results show that all the novel compounds are nontoxic to hepatic cells at 1 μ M. The same is true at 5 μ M, except for compounds **P1**, **P5**, **P6**, **P8**, and **P10**. The results show that the most potent compounds **P16** and **P17** are nontoxic at 5 μ M, with 92.18% and 95.16% viable cells. It may be concluded that the methyl-based chalcones showed a higher degree of cytotoxicity than chloro-based compounds.

Table 4. In vitro cytotoxicity of chalcones on HepG2 cells.

Compound	Viability [%]		
	1 μ M	5 μ M	25 μ M
P1	95.33 ± 2.24	62.11 ± 1.90 ^[b]	83.49 ± 1.88 ^[a]
P2	98.55 ± 2.10	93.41 ± 3.22	61.11 ± 2.16 ^[b]
P3	97.22 ± 2.06	92.26 ± 1.05	85.70 ± 1.90 ^[a]
P4	94.10 ± 2.77	94.16 ± 1.22	86.79 ± 2.03 ^[a]
P5	89.90 ± 1.53	89.61 ± 1.44 ^[a]	80.22 ± 2.08 ^[a]
P6	95.11 ± 2.34	56.58 ± 1.71 ^[b]	52.22 ± 2.17 ^[c]
P7	95.90 ± 3.02	93.55 ± 1.88	65.21 ± 2.11 ^[b]
P8	89.46 ± 2.11	89.00 ± 2.27 ^[a]	53.16 ± 2.44 ^[c]
P9	97.26 ± 2.11	95.22 ± 2.15	79.55 ± 2.14 ^[a]
P10	92.75 ± 2.61	84.33 ± 2.55 ^[a]	65.59 ± 1.37 ^[b]
P11	90.88 ± 1.36	89.90 ± 1.40	62.46 ± 1.13 ^[b]
P12	95.03 ± 2.37	90.16 ± 2.13	67.55 ± 1.71 ^[b]
P13	97.45 ± 2.03	95.33 ± 2.21	84.79 ± 1.28 ^[a]
P14	97.55 ± 1.60	95.55 ± 2.09	80.20 ± 5.66 ^[a]
P15	92.33 ± 2.69	89.16 ± 1.17	69.66 ± 1.99 ^[b]
P16	92.99 ± 2.30	92.18 ± 1.88	70.24 ± 2.55 ^[b]
P17	97.13 ± 1.71	95.16 ± 1.55	85.77 ± 1.10 ^[a]
P18	94.22 ± 2.10	90.16 ± 1.64	70.11 ± 2.37 ^[b]
P19	90.27 ± 2.42	88.91 ± 1.21	71.16 ± 1.90 ^[b]
P20	93.71 ± 1.66	90.22 ± 1.53	73.02 ± 2.13 ^[b]
moclobemide	95.70 ± 4.26	77.22 ± 2.90 ^[a]	56.20 ± 2.34 ^[b]
selegiline	95.88 ± 2.05	89.78 ± 2.60 ^[a]	60.05 ± 2.05 ^[b]
lazabemide	96.00 ± 3.85	90.25 ± 4.12 ^[a]	58.00 ± 2.91 ^[b]

Cell viability is expressed as a percentage of the control value. Data are the mean \pm SEM ($n=3$); $p < 0.05$ is considered statistically significant; [a] $p < 0.05$, [b] $p < 0.01$, [c] $p < 0.001$ versus control.

In conclusion, this study revealed a number of potent new MAO-B inhibitors among the methyl-/chloro-chalcone class of compounds. All the chalcones were found to be selective MAO-B inhibitors except the nitro-substituted compounds, which were selective inhibitors of hMAO-A. This striking selectivity profile implies that we can further develop more potent and selective hMAO-B and/or hMAO-A inhibitors from this compound class. Altogether, these compounds may qualify as starting points for the treatment of various neurodegenerative diseases such as AD and PD, resulting from the excessive production of biogenic amines.

Acknowledgements

The authors extend their appreciation to the Kerala State Council for Science, Technology & Environment (Kerala, India; application no: 01/SPS-54/2015/CSTE) for financial support.

Keywords: chalcones · docking · inhibitors · monoamine oxidase · Parkinson's disease

- [1] M. B. Youdim, D. Edmondson, K. F. Tipton, *Nat. Rev. Neurosci.* **2006**, *7*, 295–309.
- [2] J. Shih, K. Chen, M. J. Ridd, *Annu. Rev. Neurosci.* **1999**, *22*, 197–217.
- [3] B. Drukarch, F. L. van Muiswinkel, *Biochem. Pharmacol.* **2000**, *59*, 1023–1031.
- [4] H. H. Fernandez, J. J. Chen, *Pharmacotherapy* **2007**, *27*, 1745–1855.
- [5] S. Carradori, R. Silvestri, *J. Med. Chem.* **2015**, *58*, 6717–6732.
- [6] R. R. Ramsay, *Curr. Pharm. Des.* **2013**, *19*, 2529–2539.
- [7] B. Mathew, G. E. Mathew, J. Suresh, G. Ucar, R. Sasidharan, S. Anbazhagan, J. K. Vilapurathu, V. Jayaprakash, *Curr. Enzyme Inhib.* **2016**, *12*, 115–122.
- [8] A. Carlsson, *J. Neural Transm.* **2002**, *109*, 777–787.
- [9] H. Inoue, K. Castagnoli, C. Van Der Schyf, S. Mabic, K. Igarashi, N. Castagnoli, Jr., *J. Pharmacol. Exp. Ther.* **1999**, *291*, 856–864.
- [10] C. Binda, J. Wang, L. Pisani, C. Caccia, A. Carotti, P. Salvati, D. E. Edmondson, A. Mattevi, *J. Med. Chem.* **2007**, *50*, 5848–5852.
- [11] S. Henriot, C. Kuhn, R. Kettler, M. Da Prada, *J. Neural Transm. Suppl.* **1994**, *41*, 321–325.
- [12] S. Carradori, J. P. Petzer, *Expert Opin. Ther. Pat.* **2015**, *25*, 91–110.
- [13] J. P. M. Finberg, *Pharmacol. Ther.* **2014**, *143*, 133–152.
- [14] P. Singh, A. Anand, V. Kumar, *Eur. J. Med. Chem.* **2014**, *85*, 758–777.
- [15] F. Chimenti, R. Fioravanti, A. Bolasco, P. Chimenti, D. Secci, F. Rossi, M. Yáñez, F. Orallo, F. S. Alcaro, *J. Med. Chem.* **2009**, *52*, 2818–2824.
- [16] N. Morales-Camilo, C. O. Salas, C. Sanhueza, C. Espinosa-Bustos, M. Reyes-Parada, F. Gonzalez-Salas, C. Sanhauz, C. Espinosa-Bustos, S. Sepulveda-Boza, M. Reyes-Parada, F. Gonzalez-Nilo, M. Caroli-Rezende, A. Fierro, *Chem. Biol. Drug Des.* **2015**, *85*, 685–695.
- [17] J. W. Choi, B. K. Jang, N. Cho, J. H. Park, S. K. Yeon, E. J. Ju, Y. S. Lee, G. Han, A. M. Pae, D. J. Kim, K. D. Park, *Bioorg. Med. Chem.* **2015**, *23*, 6486–6496.
- [18] B. Mathew, G. E. Mathew, G. Uçar, I. Baysal, J. Suresh, J. K. Vilapurathu, A. Prakasan, J. K. Suresh, A. Thomas, *Bioorg. Chem.* **2015**, *62*, 22–29.
- [19] A. Hammuda, R. Shalaby, S. Rovida, D. E. Edmondson, C. Binda, A. Khali, *Eur. J. Med. Chem.* **2016**, *114*, 162–169.
- [20] B. Mathew, G. E. Mathew, G. Uçar, I. Baysal, J. Suresh, S. Mathew, A. Haridas, V. Jayaprakash, *Chem. Biodiversity* **2016**, *13*, 1046–1052.
- [21] B. Mathew, A. Haridas, J. Suresh, G. E. Mathew, G. Uçar, V. Jayaprakash, *Cent. Nerv. Syst. Agents Med. Chem.* **2016**, *16*, 120–136.
- [22] S. Tanaka, Y. Kuwai, M. Tabata, *Planta Med.* **1987**, *53*, 5–8.
- [23] B. Mathew, J. Suresh, G. E. Mathew, R. Parasuraman, N. Abdulla, *Cent. Nerv. Syst. Agents Med. Chem.* **2014**, *14*, 28–33.
- [24] S. J. Robinson, J. P. Petzer, A. Petzer, J. J. Bergh, A. C. U. Lourens, *Bioorg. Med. Chem. Lett.* **2013**, *23*, 4985–4989.
- [25] G. Jo, S. Ahn, B. G. Kim, H. R. Park, Y. H. Kim, H. A. Choo, D. Koh, Y. Chong, J. H. Ahn, Y. Lim, *Bioorg. Med. Chem.* **2013**, *21*, 7890–7897.
- [26] S. Zaib, S. U. F. Rizvi, S. Aslam, M. Ahmad, S. M. A. Abid, M. al-Rashida, J. Iqbal, *Med. Chem.* **2015**, *11*, 580–589.
- [27] S. Zaib, S. U. F. Rizvi, S. Aslam, M. Ahmad, M. al-Rashida, J. Iqbal, *Med. Chem.* **2015**, *11*, 497–505.
- [28] C. Minders, J. P. Petzer, A. Petzer, A. C. U. Lourens, *Bioorg. Med. Chem. Lett.* **2015**, *25*, 5270–5276.
- [29] B. Mathew, G. Uçar, S. Y. Ciftci, I. Baysal, J. Suresh, G. E. Mathew, J. K. Vilapurathu, N. A. Moosa, N. Pullarottil, L. Viswam, A. Haridas, F. Fathima, *Letts. Org. Chem.* **2015**, *12*, 605–613.
- [30] B. Mathew, A. Haridas, G. Uçar, I. Baysal, M. Joy, G. E. Mathew, B. Lakshmanan, V. Jayaprakash, *ChemMedChem* **2016**, *11*, 1161–1171.
- [31] B. Mathew, A. Haridas, G. Uçar, I. Baysal, A. A. Adeniyi, M. E. S. Soliman, M. Joy, G. E. Mathew, B. Lakshmanan, V. Jayaprakash, *Int. J. Biol. Macromol.* **2016**, *91*, 680–695.
- [32] R. Sasidharan, S. L. Manju, G. Ucar, I. Baysal, B. Mathew, *Arch. Pharm.* **2016**, *349*, 627–637.
- [33] B. Evranos-Aksöz, S. Yabanoglu-Ciftci, G. Ucar, K. Yelekci, R. Ertan, *Bioorg. Med. Chem. Lett.* **2014**, *24*, 3278–3284.
- [34] B. Evranos-Aksöz, S. Yabanoglu-Ciftci, T. Dijikic, K. Yelekci, G. Ucar, R. Ertan, *Arch. Pharm.* **2015**, *348*, 743–756.
- [35] M. C. Anderson, F. Hasan, J. M. McCrodden, K. F. Tipton, *Neurochem. Res.* **1993**, *18*, 1145–1149.
- [36] M. Yáñez, N. Fraiz, E. Cano, F. Orallo, *Biochem. Biophys. Res. Commun.* **2006**, *344*, 688–695.
- [37] F. Chimenti, E. Maccioni, D. Secci, A. Bolasco, P. Chimenti, A. Granese, S. Carradori, S. Alcaro, F. Ortuso, M. Yáñez, *J. Med. Chem.* **2008**, *51*, 4874–4880.
- [38] J. Reis, F. Cagide, D. Chavarria, T. B. Silva, C. Fernandes, A. Gaspar, E. Uriarte, F. Remiao, S. Alcaro, F. Ortuso, F. Borges, *J. Med. Chem.* **2016**, *59*, 5879–5893.
- [39] M. M. Bradford, *Anal. Biochem.* **1976**, *72*, 248–254.
- [40] A. Petzer, A. Pienaar, J. P. Petzer, *Life Sci.* **2013**, *93*, 283–287.
- [41] G. M. Morris, R. Huey, W. Lindstrom, M. F. Sanner, R. K. Belew, D. S. Goodsell, A. J. Olson, *J. Comput. Chem.* **2009**, *30*, 2785–2791.
- [42] F. Chimenti, A. Bolasco, D. Secci, P. Chimenti, A. Granese, S. Carradori, M. Yáñez, F. Orallo, F. Ortuso, S. Alcaro, *Bioorg. Med. Chem.* **2010**, *18*, 5715–5723.
- [43] R. K. Tripathi, S. Krishnamurty, S. R. Ayyannan, *ChemMedChem* **2016**, *11*, 119–132.
- [44] L. De Colibus, M. Li, C. Binda, A. Lustig, D. E. Edmondson, A. Mattevi, *Proc. Natl. Acad. Sci. USA* **2005**, *102*, 12684–12689.
- [45] B. Vishnu Nayak, S. Ciftci-Yabanoglu, S. S. Jadav, M. Jagrat, B. N. Sinha, G. Ucar, V. Jayaprakash, *Eur. J. Med. Chem.* **2013**, *69*, 762–767.
- [46] B. Mathew, J. Suresh, S. Anbazhagan, S. Dev, *Biomed. Aging Pathol.* **2014**, *4*, 297–301.
- [47] A. W. Schüttelkopf, D. M. van Aalten, *Acta Crystallogr. Sect. D* **2004**, *60*, 1355–1363.
- [48] B. V. Nayak, S. Ciftci-Yabanoglu, S. Bhakat, A. K. Timiri, B. N. Sinha, G. Ucar, M. E. S. Soliman, V. Jayaprakash, *Bioorg. Chem.* **2015**, *58*, 72–80.
- [49] M. Toprakçi, K. Yelekçi, *Bioorg. Med. Chem. Lett.* **2005**, *15*, 4438–4446.
- [50] Z. M. Wang, X. M. Li, G. M. Xue, W. Xu, X. B. Wang, L. Y. Kong, *RSC Adv.* **2015**, *5*, 104122–104137.
- [51] L. Di, E. H. Kerns, K. Fan, O. J. McConnell, G. T. Carter, *Eur. J. Med. Chem.* **2003**, *38*, 223–232.

Manuscript received: September 30, 2016

Revised: November 14, 2016

Final Article published: ■ ■ ■, 0000

COMMUNICATIONS

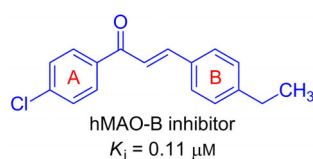
B. Mathew,* G. Uçar,* G. E. Mathew,
S. Mathew, P. Kalatharakkal Purapurath,
F. Moolayil, S. Mohan, S. Varghese Gupta



Monoamine Oxidase Inhibitory

Activity: Methyl- versus

Chloroalcone Derivatives



Me versus Cl: Twenty chalcones containing methyl and chloro substituents were synthesized and evaluated for their hMAO inhibitory activities and capacity to cross the blood–brain barrier. Chloro substitution on the A ring is more favorable for MAO-B inhibition than methyl substitution. hMAO inhibition by these chalcones was found to be reversible. The most potent inhibitor exhibited sub-micromolar activity, and is nontoxic toward cultured hepatic cells at 5–25 μM .